Journal of Computational and Applied Mathematics 388 (2021) 113244

Contents lists available at ScienceDirect

Journal of Computational and Applied Mathematics

journal homepage: www.elsevier.com/locate/cam

Computing the CEV option pricing formula using the semiclassical approximation of path integral

Axel A. Araneda [a], Marcelo J. Villena [b,*]

[a] Institute of Financial Complex Systems, Faculty of Economics and Administration, Masaryk University, Lipová 41a, 602 00 Brno, Czech Republic

[b] Faculty of Engineering & Sciences, Universidad Adolfo Ibáñez, Avda. Diagonal las Torres 2640, Peñalolén, 7941169 Santiago, Chile

ARTICLE INFO

Article history:
Received 28 November 2019
Received in revised form 8 July 2020

Keywords:
Option pricing
Constant elasticity of variance
Path integral
Semiclassical approximation
Numerical methods

ABSTRACT

The CEV model allows volatility to change with the underlying price, capturing a basic empirical regularity very relevant for option pricing, such as the volatility smile. Nevertheless, the standard CEV solution, using the non-central chi-square approach, still presents high computational times. In this paper, the CEV option pricing formula is computed using the semiclassical approximation of Feynman's path integral. Our simulations show that the method is quite efficient and accurate compared to the standard CEV solution considering the pricing of European call options.

© 2020 Elsevier B.V. All rights reserved.

1. Introduction

One of the most significant limitations of the Black–Scholes (BS) [1] model is the assumption of constant volatility, which ignores some well-known empirical regularities such as the leverage effect [2,3], and the volatility smile [4,5]. These shortcomings have inspired several non-constant volatility models in continuous time,[1] such as the 'stochastic volatility' models[2] and the 'level-dependent volatility' models[3] [10]. In the former, both the asset and the volatility have their own diffusion processes. In the level-dependent volatility models, only the asset is governed by a diffusion process, and its volatility is modeled as a function of the asset level. In this paper, the analysis will be focused on the constant elasticity of variance (CEV) model, proposed by J. Cox [11,12], without doubt, the most known level-dependent volatility approach, see [13,14] for recent applications.

As its name suggests, the Constant Elasticity of Variance option pricing model assumes that the elasticity of the variance of returns to the stock price is constant, opposed to the classical Black and Scholes model, that uses a geometric Brownian motion dynamics, where the elasticity is zero since the variance is assumed constant. Thus, the CEV model allows volatility to change with the underlying price, capturing a basic empirical regularity relevant for option pricing, such as the volatility smile [15–18]. As a consequence, the CEV model outperforms the Black–Scholes model in forecasting option prices [19–23]. Furthermore, the empirical performance of the CEV model is comparable to most stochastic volatility models, but it is considerably easier to implement and calibrate [24]. Nevertheless, the exact formula for the CEV option pricing model of a vanilla European option still involves a very complex computation of an infinite series of incomplete gamma

* Corresponding author.
E-mail address: marcelo.villena@uai.cl (M.J. Villena).

1 For discrete-time approaches to modeling volatility, see Refs. [6,7].

2 A comprehensive review for stochastic volatility models can be found in [8] and [9] .

3 A.k.a. 'local volatility'.

https://doi.org/10.1016/j.cam.2020.113244
0377-0427/© 2020 Elsevier B.V. All rights reserved.

functions [11,12]. Subsequently, Schroeder matched the Cox pricing formula with the non-central chi-square distribution, and also provides a simple approximated method for its computation [16], see Ref. [25] for a detailed derivation of the two methodologies. Since then, the use of the non-central chi-square distribution becomes the most widely used method of pricing for options under the CEV model. Besides, several alternative methods for its implementation have been developed [26–28].

Despite the advances detailed above, the standard CEV model solutions, using the non-central chi-square approach, still presents considerably high computational times, especially when: (i) the maturity is small, (ii) the volatility is low, or (iii) the elasticity of the variance tends to zero [16,29,30]. In order to deal with these problems, many alternative approaches have been reported for the European-vanilla type option pricing. These approaches include numerical schemes [29,31–33], Montecarlo simulations [34], perturbation theory model [35], and analytical approximations to the transition density [36] or to the hedging strategy [37], among others.

In this paper, the CEV option pricing formula is computed using the semiclassical approximation of Feynman's path integral. In financial literature, path integral techniques have already been used in the option pricing problem, see [38–45]. The main contribution of our paper is the use of Feynman's path integral approximation technique to a non-constant volatility model. Specifically, for the CEV model, both classical action and van Vleck determinant are derived, and several simulations are carried out in order to show the empirical potential and limitations of this technique. Our simulations show that computing the CEV option pricing formula using the semiclassical approximation of path integral is quite efficient and accurate compared to the standard CEV solution considering the pricing of European call options. Indeed, the proposed approximation reduces execution times importantly compared to the traditional solution.

In this context, we expect this research could be of importance not only because develops a novel and efficient formula for the solution of the renowned CEV model, but also because it could foster the use of the path integral's approach and its semiclassical approximation as an interesting computational tool to deal efficiently with other complex problems in quantitative finance.

The structure of the paper is the following. Firstly, Feynman's path integral formulation is revisited. Secondly, the path integral approximation is applied to the basic BS model. Thirdly, the path integral approximation is applied to the CEV model. Later, a numerical solution to the CEV model is developed. In the next section, several numerical simulations are carried out in order to measure the performance of the new method, comparing the path integral approximation with the traditional non-central chi-squared approach for the pricing of European call options. Finally, some conclusions and future research avenues are outlined.

2. The Feynman path integral approach

The path integral formalism was developed by Richard P. Feynman [46], introducing the action principle from classical mechanics to quantum mechanics. Nowadays Feynman's path integral is a well-known tool in quantum mechanics, and statistical and mathematical physics, with applications in many branches of physics such as optics, thermodynamics, nuclear physics, atomic and molecular physics, cosmology, polymer science and other interdisciplinary areas [47–49]

In the following lines, we describe the fundamentals of the path integral methodology. The starting point is the time-dependent Schrödinger equation:

$$i\hbar\frac{\partial\Psi(x,t)}{\partial\tilde{t}} = \hat{\mathrm{H}}\Psi(x,t) \tag{1}$$

where Ψ is the wave function and $\hat{\mathrm{H}}$ the Hamiltonian quantum operator (for this instance we consider a time independent Hamiltonian).

Considering $\Psi_0(x)$ as the initial value of Ψ (i.e., $\Psi(x,t=0)=\Psi_0(x)$), the general solution of Eq. (16) is given by:

$$\Psi(x,t) = e^{-i\hat{\mathrm{H}}t/\hbar}\Psi_0(x) \tag{2}$$

Equivalently, using convolution properties, the value at time t of the wave function is represented by:

$$\begin{aligned}\Psi(x,t) &= \int_{-\infty}^{\infty} \mathrm{e}^{-i\hat{\mathrm{H}}t/\hbar}\delta\left(x-x_0\right)\Psi_0\left(x_0\right)\mathrm{d}x_0 \\ &= \int_{-\infty}^{\infty} K\left(x,t\mid x_0,0\right)\Psi_0\left(x_0\right)\mathrm{d}x_0\end{aligned} \tag{3}$$

where $K\left(x,t|x_0,0\right) =< x_0|e^{-it\hat{\mathrm{H}}/\hbar}|x >$ is called the propagator.

Feynman concentrated on a previous work of Dirac [50], related with the proportionality between the exponential of the action over the classical path (which come from the Lagrangian formalism) and the propagator in quantum mechanics:

$$K\left(x,t\mid x_0,0\right) \propto \mathrm{e}^{(i/\hbar)A[x_{cl}]}$$

where A is the action functional, defined as the time integral Lagrangian:

$$A[x(t)] = \int_0^t \mathcal{L}(x,\dot{x},t')\mathrm{d}t'$$

and $A\left[x_{cl}\right]$ indicates that the action is evaluated over the classical trajectory from x_0 to x.

Feynman reformulated Dirac formulation and described the propagator as the contributions of the all virtual paths, not only the classical ones:

$$K\left(x,t\mid x_0,0\right)=\sum_{\substack{\text{All Paths}\\ \text{from } x_0 \text{ to } x}}\tilde{\mathcal{N}}\mathrm{e}^{(i/\hbar)A[x(t)]}$$

where $\tilde{\mathcal{N}}$ is an appropriated normalization for K.

Thus, using the Riemann integral for each path (see Ref. [47]), the propagator is defined as:

$$K\left(x,t\mid x_0,0\right)=\int\mathcal{D}[x(t)]\mathrm{e}^{(i/\hbar)A[x(t)]} \tag{4}$$

The functional integral of the right-hand side of Eq. (4) is defined as a 'Path Integral', and the measure of the integration is given by $\mathcal{D}[x(t)]$ which means the integrations over all the trajectories.

The standard computation of the path integral is done via the time-slicing scheme [46,47], which is not a straightforward procedure. Nevertheless, there is an alternative and popular method used in physics called the 'semiclassical approximation', which approximates the argument of the path integral into a Gaussian function, arriving this way to a solution in terms of the classical path, see [51–53]. The general procedure is explained below.

First, we write the path that links the points $x(t_0)=x_0$ with $x(t_1)=x_1$ as the classical trajectories as the main contribution plus the fluctuations around it:

$$x(t)=x(t)_{cl}+\delta x(t) \tag{5}$$

with the fixed conditions (extremality condition):

$$\delta x(t_0)=\delta x(t_1)=0 \tag{6}$$

Later, we can expand the action around to $x_{cl}(t)$ using a functional Taylor series [54]:

$$\begin{aligned}A\left[x(t)_{cl}+\delta x\right]=A\left[x(t)\right]\Big|_{x_{cl}(t)}&+\int_{t_0}^{t_1}\mathrm{d}t\frac{\delta A\left[x(t)\right]}{\delta x(t)}\Big|_{x_{cl}(t)}\delta x(t)\\&+\frac{1}{2}\int_{t_0}^{t_1}\mathrm{d}t\mathrm{d}t'\frac{\delta^2A}{\delta x(t)\delta x(t')}\delta x(t)\delta x(t')\Big|_{x_{cl}(t)}\\&+\frac{1}{3!}\int_{t_0}^{t_1}\mathrm{d}t\mathrm{d}t'\mathrm{d}t''\frac{\delta^3A}{\delta x(t)\delta x(t')\delta x(t'')}\delta x(t)\delta x(t')\delta x(t'')\Big|_{x_{cl}(t)}+\mathcal{O}(4)\end{aligned} \tag{7}$$

The semiclassical approximation consists in truncated up to the quadratic terms the expansion (7):

$$A\left[x(t)\right]\approx A\left[x_{cl}(t)\right]+\frac{1}{2}\int_{t_0}^{t_1}\frac{\delta^2A}{\delta x(t)\delta x(t')}\delta x(t)\delta x(t')\Big|_{x_{cl}(t)}$$

where the linear term is vanished due to the extremality condition.

Thus, the propagator in the semiclassical limit becomes:

$$\begin{aligned}K^{SC}\left(x_1,t_1|x_0,t_0\right)&=\mathrm{e}^{(i/\hbar)A[x_{cl}(t)]}\int\mathcal{D}\left[\delta x\right]\mathrm{e}^{(i/\hbar)\frac{1}{2}\int_{t_0}^{t_1}\frac{\delta^2A}{\delta x(t)\delta x(t')}\delta x(t)\delta x(t')\Big|_{x_{cl}(t)}}\\&=\mathrm{e}^{(i/\hbar)A[x_{cl}(t)]}\mathcal{N}\end{aligned} \tag{8}$$

where $\mathcal{N}$ is a normalization which incorporates the contribution of the second order term, defined by a Gaussian path integral . An analytical expression was developed for it in Ref. [55] as the necessary condition to maintain the unitary measure of the probability amplitudes [56], and it is equal to:

$$\mathcal{N}=\sqrt{-\frac{\mathcal{M}}{2\pi}} \tag{9}$$

where $\mathcal{M}$ is the van Vleck–Pauli–Morette determinant[4] [55,58], computed as:

$$\mathcal{M}=\frac{\partial^2A\left[x_{cl}\right]}{\partial x_0\partial x_1} \tag{10}$$

[4] A.k.a Morette–Van Hove determinant. See Ref. [57] for details.

Finally, in the semiclassical regime, the propagator becomes[5]:

$$K(x,t \mid x_0,0) = \sqrt{-\frac{\mathcal{M}}{2\pi}}\, e^{\frac{i}{\hbar}A[x_{cl}]} \tag{11}$$

The only necessary condition to get a solution for Eq. (11) is to have an analytical expression for the action over the classical path. This can be achieved via the Hamilton equations (or Euler–Lagrange equation) using the classical Hamiltonian related to the quantum Hamiltonian defined in Eq. (1).

Finally, two important notes must be considered in relation to the semiclassical approximation [48]:

(i) It is exact if the Lagrangian is quadratic.
(ii) It satisfy the Schrödinger equation up to terms of order $\hbar^2$.

In the next section, we apply the semiclassical approximation of path integral to the European-vanilla type option pricing, arriving to the famous Black–Scholes model.

3. A semiclassical approximation of the path integral approach to the Black–Scholes model

We assume stochastic spot prices S_t, governing by a standard geometric Brownian motion under risk-neutral $\mathbb{Q}$-measure:

$$\frac{dS_t}{S_t} = r\,dt + \sigma\,dW_t \tag{12}$$

where W_t is a standard Gauss–Wiener process with variance t. The parameters r and σ are the risk-free rate of interest and the volatility of the return, respectively. At this stage, we set these parameters as constants.

By Itô's calculus, is possible to rewrite Eq. (12) into:

$$d(\ln S_t) = \left(r - \frac{\sigma^2}{2}\right)dt + \sigma\,dW_t \tag{13}$$

and labeling $x_t = \ln S_t$:

$$dx_t = \left(r - \frac{\sigma^2}{2}\right)dt + \sigma\,dW_t \tag{14}$$

The probability density $P(x_t, t, x', t')$ for the random variable x_t evolves according to the Fokker–Planck (or forward Kolmogorov) equation [59]:

$$\begin{aligned}\frac{\partial P}{\partial t} &= -\frac{\partial}{\partial x}\left[\left(r - \frac{\sigma^2}{2}\right)P\right] + \frac{1}{2}\frac{\partial^2}{\partial x^2}\left(\sigma^2 P\right)\\ &= \frac{1}{2}\sigma^2\frac{\partial^2 P}{\partial x^2} - \left(r - \frac{\sigma^2}{2}\right)\frac{\partial P}{\partial x}\end{aligned} \tag{15}$$

with initial condition:

$$P(x_t, t=0) = \delta(x)$$

Using the wick rotation ($\tilde{t} = it$), the evolution of the probability density P (Eq. (15)) can be mapped to the Schödringer equation:

$$i\hbar\frac{\partial \Psi}{\partial \tilde{t}} = \hat{H}_{BS}\Psi \tag{16}$$

where the wave function Ψ represents the probability P, and the quantum Hamiltonian $\hat{H}_{BS}$, namely for this instance the Black–Scholes Hamiltonian, is given by [60]:

$$\hat{H}_{BS} = \frac{1}{2}\sigma^2\frac{\partial^2}{\partial x^2} - \left(r - \frac{\sigma^2}{2}\right)\frac{\partial}{\partial x}$$

In order to ensure the compatibility between Eqs. (15) and (16), we need to set $\hbar = 1$.

Given the momentum operator $\hat{p} = -i\hbar\frac{\partial}{\partial x} = -i\frac{\partial}{\partial x}$, the Hamiltonian can be expressed as :

$$\hat{H}_{BS} = -\frac{1}{2}\sigma^2\hat{p}^2 - i\left(r - \frac{\sigma^2}{2}\right)\hat{p}$$

[5] Eq. (11) is called the Pauli formula [48].

Considering $\Psi_0(x)$ as the initial value of Ψ (i.e., $\Psi(x, t = 0) = \Psi_0(x)$), the general solution of Eq. (16) is given by (see [41]):

$$\begin{aligned}\Psi(x,t) &= e^{-i\hat{H}_{BS}\tilde{t}}\Psi_0(x)\\ &= e^{\hat{H}_{BS}t}\Psi_0(x)\end{aligned}$$

Equivalently, using the convolution properties, the value at time t_0 of the wave function is represented by:

$$\Psi(x,t_0) = \int_{-\infty}^{\infty} K_{BS}\left(x_T, T|x_0, t_0\right)\Psi_T\left(x_T\right)\mathrm{d}x_T$$

where $K_{BS}\left(x_T, T|x_0, t_0\right)$ is the propagator, which admits the following path integral representation in euclidean time [47]:

$$K_{BS}\left(x_T, T|x_0, t_0\right) = \int \mathcal{D}x(t)e^{-S_{BS}[x(t)]}$$

being $S_{BS}\left[x(t)\right]$ the euclidean classical action which links the points and $x(t_0) = x_0$ and $x\left(T\right) = x_T$; defined by:

$$S_{BS}\left[x(t)\right] = \int_{t_0}^{T}\mathcal{L}_{BS}dt$$

where $\mathcal{L}_{BS}$ is the Black–Scholes Lagrangian.

In order to obtain an expression for the propagator (Eqs. (8)–(11)) we request the classical action evaluated over the classical path. This can be obtained using classical Hamiltonian mechanics.

The classical Hamiltonian $\mathcal{H}_{BS}$ associated to the operator $\hat{\mathrm{H}}_{BS}$ is:

$$\mathcal{H}_{BS} = -\frac{1}{2}\sigma^2p^2 - i\left(r - \frac{\sigma^2}{2}\right)p$$

with its related classical Hamilton's equations in euclidean time:

$$\begin{aligned}-i\dot{x} &= \frac{\partial\mathcal{H}_{BS}}{\partial p}\\ -i\dot{p} &= -\frac{\partial\mathcal{H}_{BS}}{\partial x}\end{aligned}$$

or explicitly:

$$p = \frac{i}{\sigma^2}\left[\dot{x} - \left(r - \frac{\sigma^2}{2}\right)\right] \tag{17}$$

$$\dot{p} = 0 \tag{18}$$

Then, the Lagrangian is given via the Legendre transformation:

$$\begin{aligned}\mathcal{L}_{BS} &= -ip\dot{x} - \mathcal{H}_{BS}\\ &= -ip\dot{x} + \frac{1}{2}\sigma^2p^2 + i\left(r - \frac{\sigma^2}{2}\right)p\\ &= \frac{p}{2}\left[\sigma^2p - 2i\left(\dot{x} - r + \frac{\sigma^2}{2}\right)\right]\end{aligned}$$

Using the values that solves the Hamilton's equation (Eqs. (17)–(18)), the Lagrangian is:

$$\mathcal{L}_{BS} = \frac{1}{2\sigma^2}\left[\dot{x} - \left(r - \frac{\sigma^2}{2}\right)\right]^2 \tag{19}$$

Later, the Euler–Lagrange equation:

$$\frac{\mathrm{d}}{\mathrm{d}t}\left(\frac{\partial\mathcal{L}_{BS}}{\partial\dot{x}}\right) - \frac{\partial\mathcal{L}_{BS}}{\partial x} = 0 \tag{20}$$

yields to the free particle Newton equation:

$$\ddot{x} = 0 \tag{21}$$

which leads to the classical path:

$$\dot{x} = C \tag{22}$$

$$x = Ct + D \tag{23}$$

The values for C and D are obtained using the boundary conditions (fixed values) for x, $x(t_0) = x_0$ and $x\left(T\right) = x_T$.

Thus, the classical path, with $t_0 \leq t \leq T$, is described by:

$$\dot{x}(t) = \frac{x_T - x_0}{T - t_0} \tag{24}$$

$$x(t) = \frac{x_T - x_0}{T - t_0}(t - t_0) + x_0 \tag{25}$$

Then, using Eqs. (24) and (25), the corresponding classical action over the classical path:

$$\begin{aligned} A\left[x_{class}(t)\right] &= \int_t^T \frac{1}{2\sigma^2}\left[\dot{x}(t') - \left(r - \frac{\sigma^2}{2}\right)\right]^2 \mathrm{d}(t') \\ &= \frac{1}{2\sigma^2(T - t_0)}\left[(x_T - x_0) - (T - t_0)\left(r - \frac{\sigma^2}{2}\right)\right]^2 \end{aligned} \tag{26}$$

Now, we are in conditions to compute the propagator. According to Eqs. (9)–(10):

$$\mathcal{N} = \frac{1}{\sqrt{2\pi\sigma^2(T - t_0)}}$$

and the semiclassical approximation for the propagator becomes:

$$\begin{aligned} K_{BS}^{SC}(x_T, T|x_0, t_0) &= \frac{e^{-S_{BS}[x_{class}(t)]}}{\sqrt{2\pi\sigma^2(T - t_0)}} \\ &= \frac{1}{\sqrt{2\pi\sigma^2(T - t_0)}} e^{-\frac{1}{2\sigma^2(T - t_0)}\left[(x_T - x_0) - (T - t_0)\left(r - \frac{\sigma^2}{2}\right)\right]^2} \end{aligned}$$

Then, the wave function solution is reduced to:

$$\Psi(x, t_0) = \frac{1}{\sqrt{2\pi\sigma^2(T - t_0)}} \int_{-\infty}^{\infty} e^{-S_{BS}[x_{class}(t)]} \Psi_T(x_T)\, \mathrm{d}x_T \tag{27}$$

$$= \frac{1}{\sqrt{2\pi\sigma^2(T - t_0)}} \int_{-\infty}^{\infty} e^{-\frac{1}{2\sigma^2(T - t_0)}\left[(x_T - x_0) - (T - t_0)\left(r - \frac{\sigma^2}{2}\right)\right]^2} \Psi_T(x_T)\, \mathrm{d}x_T \tag{28}$$

which is equal to the convolution between the propagator and the contract function:

$$\Psi(x, t_0) = K_{SC}^{BS} * \Psi_T(x_T)$$

The solution of Eq. (27) depends on the boundary condition Ψ_T (contract function). We analyze the case of a European call option, i.e.,:

$$\begin{aligned} \Psi_T(x_T) &= e^{-r\tau} \max\{S_T - E, 0\} \\ &= e^{-r\tau} \max\left\{e^{x_T} - E, 0\right\} \end{aligned}$$

being E the strike price.

Then, the wave function for this case is:

$$\begin{aligned} \Psi(x, t) &= \frac{e^{-r(T - t_0)}}{\sqrt{2\pi\sigma^2(T - t_0)}} \int_{\ln E}^{\infty} e^{-\frac{1}{2\sigma^2(T - t_0)}\left[(x_T - x_0) - (T - t_0)\left(r - \frac{\sigma^2}{2}\right)\right]^2} \left(e^{x_T} - E\right) \mathrm{d}x_T \\ &= \frac{e^{-r(T - t_0)}}{\sqrt{2\pi\sigma^2(T - t_0)}} \int_{\ln E}^{\infty} e^{x_T} e^{-\frac{1}{2\sigma^2(T - t_0)}\left[(x_T - x_0) - (T - t_0)\left(r - \frac{\sigma^2}{2}\right)\right]^2} \mathrm{d}x_T \\ &\quad - \frac{E e^{-r(T - t_0)}}{\sqrt{2\pi\sigma^2(T - t_0)}} \int_{\ln E}^{\infty} e^{-\frac{1}{2\sigma^2(T - t_0)}\left[(x_T - x_0) - (T - t_0)\left(r - \frac{\sigma^2}{2}\right)\right]^2} \mathrm{d}x_T \\ &= I_1 - I_2 \end{aligned}$$

Developing I_1, we have:

$$\begin{aligned} I_1 &= \frac{e^{-r(T - t_0)}}{\sqrt{2\pi\sigma^2(T - t_0)}} \int_{\ln E}^{\infty} e^{-\frac{1}{2\sigma^2(T - t_0)}\left[x_T^2 - 2x_T\left(x_0 + (T - t_0)\left(r - \frac{\sigma^2}{2}\right)\right) + \left(x_0 + (T - t_0)\left(r - \frac{\sigma^2}{2}\right)\right)^2\right] + x_T} \mathrm{d}x_T \\ &= \frac{e^{x_0}}{\sqrt{2\pi\sigma^2(T - t_0)}} \int_{\ln E}^{\infty} e^{-\frac{1}{2\sigma^2(T - t_0)}\left[x_T - \left(x_0 + (T - t_0)\left(r + \frac{\sigma^2}{2}\right)\right)\right]^2} \mathrm{d}x_T \end{aligned}$$

Carrying out the change of variable $u = \left[-x_T + x_0 + (T-t_0)\left(r+\frac{\sigma^2}{2}\right)\right]/\sqrt{\sigma^2(T-t_0)}$, and replacing $x_0 = \ln S_0$, we have:

$$\begin{aligned} I_1 &= -S_0\left[\int_{x_0-\ln E+(T-t_0)\left(r+\frac{\sigma^2}{2}\right)}^{-\infty} e^{-\frac{1}{2}v^2}\mathrm{d}u\right] \\ &= S_0 N(d_1) \end{aligned}$$

where $N(\cdot)$ is the standard normal cumulative function and $d_1 = \frac{\ln\left(\frac{S_0}{E}\right)+(T-t_0)\left(r+\frac{\sigma^2}{2}\right)}{\sqrt{\sigma^2(T-t_0)}}$.

To solve I_2 we use the change of variable $v = -\left[(x_T - x_0) - (T-t_0)\left(r-\frac{\sigma^2}{2}\right)\right]/\sqrt{\sigma^2(T-t_0)}$, so:

$$\begin{aligned} I_2 &= -\frac{Ee^{-r(T-t)}}{\sqrt{2\pi}}\int_{x_0-\ln E+(T-t_0)\left(r-\frac{\sigma^2}{2}\right)}^{-\infty} e^{-\frac{1}{2}v^2}\mathrm{d}u \\ &= Ee^{-r(T-t)}N(d_2) \end{aligned}$$

being $d_2 = \frac{\ln\left(\frac{S_0}{E}\right)+(T-t_0)\left(r-\frac{\sigma^2}{2}\right)}{\sqrt{\sigma^2(T-t_0)}} = d_1 - \sqrt{\sigma^2(T-t_0)}$.

Finally, the price of a call option at time t_0, using the path integral formulation, is given by:

$$\Psi(S_0, t_0) = S_0 N(d_1) - Ee^{-r(T-t_0)}N(d_2)$$

which is exactly the same value obtained by Black–Scholes [1] for a European call option. [6]

4. A semiclassical approximation of the path integral approach to the CEV model

In the CEV model, under the risk-neutral measure, the asset is governed by the following stochastic differential equation [11,12]:

$$\mathrm{d}S(S,t) = rS\mathrm{d}t + \sigma S^{\frac{\alpha}{2}}\mathrm{d}W \tag{29}$$

being r the constant risk-free of interest, σ and α constant values, and W a standard Wiener process, with $\mathrm{d}W \sim N(0, \mathrm{d}t)$. In its paper, Cox imposed the domain for α in the range $[0, 2[$. In this interval, the asset's volatility is negatively correlated with the asset's returns. (leverage effect). For values greater than two, the process described in Eq. (29) is not a martingale [61,62] (i.e, there are not a unique risk-neutral measure). For $\alpha < 0$, the volatility unrealistically goes to zero as S increases [63]. Then, the same Cox's condition for α is assumed in this paper.

The process described by Eq. (29) can be interpreted as a generalization of the standard geometric Brownian motion used in the Black–Scholes model [1], but considering a non-constant local volatility function equals to $\sigma S^{\frac{\alpha-2}{2}}$. In fact, for the limit case $\alpha = 2$, Eq. (29) is degenerated to the BS case [64]. Also, the CEV model has correspondence with other approaches: For $\alpha = 1$, it becomes a square root process, addressed by Cox and Ross [65]; and for $\alpha = 0$, S follows an Ornstein–Uhlenbeck type process [66].

The CEV model described in Eq. (29) owes its name to the fact that the variance of the return is given by:

$$\begin{aligned} v &= \mathrm{var}\left(\frac{\mathrm{d}S}{S}\right) \\ &= \mathrm{var}\left(r\mathrm{d}t + \sigma S^{\frac{\alpha-2}{2}}\mathrm{d}W\right) \\ &= \sigma^2 S^{\alpha-2}\mathrm{d}t \end{aligned}$$

and then, the elasticity of the variance with respect to the spot:

$$\frac{\mathrm{d}v/v}{\mathrm{d}S/S} = \alpha - 2$$

is constant.

The strategy to get an option pricing formula will be the same that it was developed in Section 3. That is: (i) we arrive at the Fokker–Planck equation; (ii) we rewrite it as a Schrödinger equation; (iii) later, we find the classical path through the Hamilton or Euler–Lagrange equations, working with the propagator as a path integral, (iv) we evaluate the classical path using semiclassical arguments; and (v) finally, we compute the convolution between the propagator and the contract function in the integral form.

6 As noted previously (On page 2), the semiclassical approximation is exact if the Lagrangian is quadratic, as in the case of the B-S Lagrangian (Eq. (19)).

Firstly, we use the following transformation:

$$y(S,t) = S^{2-\alpha}$$

and by the Itô's Lemma, Eq. (29) can be rewritten as:

$$\mathrm{d}y = (2-\alpha)\left[ry + \frac{1}{2}(1-\alpha)\sigma^2\right]\mathrm{d}t + (2-\alpha)\sigma\sqrt{y}\mathrm{d}W$$

The Fokker–Planck equation rules the transition probability $P(y,t)$ of the variable y. Thus:

$$\begin{aligned}\frac{\partial P}{\partial t} &= \frac{1}{2}\frac{\partial^2}{\partial y^2}\left[(2-\alpha)^2\sigma^2 yP\right] - \frac{\partial}{\partial y}\left[(2-\alpha)\left(ry + \frac{1}{2}(1-\alpha)\sigma^2\right)P\right] \\ &= \frac{1}{2}\beta^2\sigma^2 y\frac{\partial^2 P}{\partial y^2} + \beta r[\gamma - y]\frac{\partial P}{\partial y} - \beta rP \end{aligned} \tag{30}$$

being β and γ constant values (parameters), defined as:

$$\beta = 2-\alpha \qquad\qquad \gamma = \frac{3-\alpha}{2r}\sigma^2$$

The relationship (30) can be interpreted as the Schrödinger equation in Euclidean (Wick-rotated) time, with $\hbar = 1$:

$$\frac{\partial \Psi}{\partial t} = \hat{\mathrm{H}}\Psi$$

where the wave function Ψ is equivalent to the probability P and the Hamiltonian operator $\hat{\mathrm{H}}$ is given by:

$$\hat{\mathrm{H}} = \frac{1}{2}\beta^2\sigma^2 y\frac{\partial^2}{\partial y^2} + \beta r[\gamma - y]\frac{\partial}{\partial y} - \beta r$$

Using the quantum momentum operator, $\hat{p} = -i\frac{\partial}{\partial y}$, the Hamiltonian goes to:

$$\hat{\mathrm{H}} = -\frac{1}{2}\beta^2\sigma^2 y\hat{p}^2 + i\beta r[\gamma - y]\hat{p} - \beta r$$

Later, we consider a final term condition (contract function) of the form:

$$\Psi(y, t = T) = \Psi(y_T)$$

The wave function Ψ, can be written in terms of its propagator K:

$$\Psi(y, t_0) = \int_{-\infty}^{\infty} K(y_T, 0|y_0, 0)\,\Psi(y_T)\mathrm{d}y_T$$

where the propagator can be estimated using the path integral:

$$K(y_T, T|y_0, 0) = \int \mathcal{D}[y(t)]\, e^{-S[y(t)]}$$

being $\mathcal{D}[y(\tau)]$ the infinitesimal contribution of all the paths that satisfies the boundary conditions $y(t = T) = y_T$ and $y(t = 0) = y_0$; being S the euclidean classical action.

Using semiclassical arguments the propagator becomes:

$$K(y_T, T|y_0, 0) = e^{-A[y_{cl}(t)]}\sqrt{-\frac{1}{2\pi}\mathcal{M}}$$

The classical path is obtained as the solution of the Hamilton equations. The classical Hamiltonian $\mathcal{H}$ related to $\hat{\mathrm{H}}$ is:

$$\mathcal{H} = -\frac{1}{2}\beta^2\sigma^2 yp^2 + i\beta r[\gamma - y]p - \beta r$$

where p represents the classical momentum. Considering the Hamilton equation in Euclidean time, the momentum can be written in terms of y and $\dot{y}$:

$$p = i\frac{\dot{y} + \beta r[\gamma - y]}{\beta^2\sigma^2 y} \tag{31}$$

So, using Eq. (31), the Lagrangian takes the form:

$$\begin{aligned}\mathcal{L} &= -i\dot{y}p - \mathcal{H} \\ &= \frac{\{\dot{y} + \beta r[\gamma - y]\}^2}{2\beta^2\sigma^2 y} + Ar\end{aligned} \tag{32}$$

The unique classical trajectory is which obeys the Euler–Lagrange equation:

$$\frac{\mathrm{d}}{\mathrm{d}t}\left(\frac{\partial \mathcal{L}}{\partial \dot{y}}\right)-\frac{\partial \mathcal{L}}{\partial y}=0 \tag{33}$$

Computing the derivatives:

$$\begin{aligned}\frac{\partial \mathcal{L}}{\partial \dot{y}} &= \frac{\dot{y}+\beta r\left(\gamma-y\right)}{\beta^2\sigma^2 y}\\ \frac{\mathrm{d}}{\mathrm{d}t}\left(\frac{\partial \mathcal{L}}{\partial \dot{y}}\right) &= \frac{\ddot{y}y-\dot{y}^2-\beta\gamma r\dot{y}}{\beta^2\sigma^2 y^2}\\ \frac{\partial \mathcal{L}}{\partial y} &= -\frac{\left[\dot{y}+\beta r\left(\gamma+y\right)\right]\left[\dot{y}+\boldsymbol{\beta} r\left(\gamma-y\right)\right]}{2\beta^2\sigma^2 y^2}\end{aligned}$$

and replacing into Eq. (33), we have a second order differential equation that rules the classical behavior of $y(t)$:

$$2y\ddot{y}-\dot{y}^2+\beta^2 r^2\left(\gamma^2-y^2\right)=0 \tag{34}$$

Then, solving Eq. (34), the classical path is given by:

$$y_{cl}\left(t'\right)=\frac{\left(C_1+2C_2e^{-rt'\beta}\right)^2-\gamma^2}{4C_2e^{-rt'\beta}} \tag{35}$$

being C_1 and C_2 constants given by the fixed values of the path at time $t'=0$ and $t'=T$ (i.e., y_0 and y_T, respectively): which yields to:

$$C_1=\frac{\left(e^{rT\beta}+1\right)\sqrt{\gamma^2\left(e^{rT\beta}-1\right)^2+4y_0y_Te^{rT\beta}}-2e^{rT\beta}\left(y_0+y_T\right)}{\left(e^{r\tau\beta}-1\right)^2} \tag{36}$$

$$C_2=\frac{\left[y_Te^{rT\beta}+y_0-\sqrt{\gamma^2\left(e^{rT\beta}-1\right)^2+4y_0y_Te^{rT\beta}}\right]}{\left(e^{rT\beta}-1\right)^2} \tag{37}$$

Later, using Eq. (35), the Lagrangian over the classical path is:

$$\begin{aligned}\mathcal{L}_{cl} &= \mathcal{L}\left[y_{cl}\right]\\ &= \frac{r^2\left(C_1+2C_2e^{rt'\beta}+\gamma\right)\left(\gamma-C_1\right)^2}{2\sigma^2C_2e^{rt'\beta}\left(C_1+2C_2e^{rt'\beta}-\gamma\right)}+\beta r\end{aligned} \tag{38}$$

Thus the classical action is obtained by time integration of Eq. (38) :

$$\begin{aligned}A_{cl} &= \int_{t'=t_0}^{t'=T}\mathcal{L}_{cl}dt'\\ &= \frac{r}{\sigma^2}\left\{\beta\sigma^2t'-2\gamma rt'+\frac{2\gamma}{\beta}\ln\left[\gamma-\left(C_1+2C_2\mathrm{e}^{rt'\beta}\right)\right]+\frac{\left(\gamma^2-C_1^2\right)}{2A\beta\mathrm{e}^{rt'\beta}}\right\}\Bigg|_{t'=0}^{t'=T}\\ &= \beta rT-\frac{2\gamma r^2}{\sigma^2}\tau+\frac{2\gamma r}{\beta\sigma^2}\ln\left[\frac{\gamma-\left(C_1+2C_2\mathrm{e}^{rT\beta}\right)}{\gamma-\left(C_1+2C_2\right)}\right]\\ &\quad+\frac{\left(\gamma^2-C_1^2\right)}{2\beta C_2\mathrm{e}^{rT\beta}}\left(1-\mathrm{e}^{rT\beta}\right)\end{aligned} \tag{39}$$

So, using Eq. (39), the van Vleck determinant (Eq. (10)) is computed as :

$$\begin{aligned}\mathcal{M} = \frac{2\gamma r\left[\gamma-\left(C_1+2C_2\right)\right]}{\beta\sigma^2\left[\gamma-\left(C_1+2C_2\mathrm{e}^{r\tau\beta}\right)\right]}&\left\{\frac{-\frac{\partial^2}{\partial y_0\partial y_T}\left(C_1+2C_2\mathrm{e}^{rT\beta}\right)}{\gamma-\left(C_1+2C_2\right)}\right.\\ &\left.-\frac{\left[\frac{\partial}{\partial y_0}\left(C_1+2C_2\right)\right]\left[\frac{\partial}{\partial y_T}\left(C_1+2C_2\mathrm{e}^{rT\beta}\right)\right]+\left[\frac{\partial}{\partial y_T}\left(C_1+2C_2\right)\right]\left[\frac{\partial}{\partial y_0}\left(C_1+2C_2\mathrm{e}^{rT\beta}\right)\right]}{\left[\gamma-\left(C_1+2C_2\right)\right]^2}\right.\end{aligned}$$

$$+\frac{2\left[\gamma-\left(C_1+2C_2e^{rT\beta}\right)\right]\left[\frac{\partial}{\partial y_T}\left(C_1+2C_2\right)\right]\left[\frac{\partial}{\partial y_0}\left(C_1+2C_2\right)\right]}{\left[\gamma-\left(C_1+2C_2\right)\right]^3}$$
$$+\frac{\left[\gamma-\left(C_1+2C_2e^{rT\beta}\right)\right]\left[\frac{\partial^2}{\partial y_0\partial y_T}\left(C_1+2C_2\right)\right]}{\left[\gamma-\left(C_1+2C_2\right)\right]^2}\Bigg\}$$
$$-\Bigg\{\frac{2\gamma r\left[\gamma-\left(C_1+2C_2\right)\right]\left[-\frac{\partial}{\partial y_0}\left(C_1+2C_2e^{rT\beta}\right)\right]}{\beta\sigma^2\left[\gamma-\left(C_1+2C_2e^{rT\beta}\right)\right]^2}$$
$$\times\left[\frac{-\frac{\partial}{\partial y_T}\left(C_1+2C_2e^{rT\beta}\right)}{\gamma-\left(C_1+2C_2\right)}+\frac{\left[\gamma-\left(C_1+2C_2e^{rT\beta}\right)\right]\left[\frac{\partial}{\partial y_T}\left(C_1+2C_2\right)\right]}{\left[\gamma-\left(C_1+2C_2\right)\right]^2}\right]\Bigg\}$$
$$+\frac{2\gamma r\left[-\frac{\partial}{\partial y_0}\left(C_1+2C_2\right)\right]}{\beta\sigma^2\left[\gamma-\left(C_1+2C_2e^{rT\beta}\right)\right]}\Bigg\{\frac{\left[\gamma-\left(C_1+2C_2e^{rT\beta}\right)\right]\left[\frac{\partial}{\partial y_T}\left(C_1+2C_2\right)\right]}{\left[\gamma-\left(C_1+2C_2\right)\right]^2}$$
$$\frac{-\frac{\partial}{\partial y_T}\left(C_1+2C_2e^{rT\beta}\right)}{\gamma-\left(C_1+2C_2\right)}\Bigg\}+\frac{r\left(e^{\beta rT}-1\right)\left[\left(\frac{\partial C_1}{\partial y_0}\right)\left(\frac{\partial C_1}{\partial y_T}\right)+\frac{\partial^2 C_1}{\partial y_0\partial y_T}\right]}{\beta\sigma^2C_2e^{rT\beta}}$$
$$-\frac{r\left(e^{\beta rT}-1\right)\left[\left(\frac{\partial C_1}{\partial y_T}\right)\left(\frac{\partial C_2}{\partial y_0}\right)+\left(\frac{\partial C_1}{\partial y_0}\right)\left(\frac{\partial C_2}{\partial y_T}\right)-\frac{1}{2}\left(\gamma^2-C_1^2\right)\left(\frac{\partial^2 C_2}{\partial y_0\partial y_T}\right)\right]}{\beta\sigma^2C_2^2e^{rT\beta}}$$
$$-\frac{r\left(e^{\beta rT}-1\right)\left(\gamma^2-C_1^2\right)\left(\frac{\partial C_2}{\partial y_T}\right)\left(\frac{\partial C_2}{\partial y_0}\right)}{\beta\sigma^2C_2^3e^{rT\beta}}$$

Then is possible to compute the semiclassical propagator, through the Euclidean form of the Pauli's formula (Eq. (11)):

$$K=e^{-A[y_{cl}(t)]}\sqrt{-\frac{1}{2\pi}\mathcal{M}}$$

Finally, the value of the wave function at time $t=0$, is given by:

$$\Psi\left(y_0,0\right)=\sqrt{\frac{1}{2\pi}}\int_{-\infty}^{\infty}\sqrt{-\mathcal{M}}e^{-A_{cl}}\Psi(y_T)\mathrm{d}y_T$$

Coming back to the option pricing problem, if we consider a European call option, with strike E and maturity T, the value of the option at time t under the CEV model will be:

$$C\left(S_0,0\right)=\sqrt{\frac{1}{2\pi}}\int_{E^{1/(2-\alpha)}}^{\infty}\sqrt{-\mathcal{M}}e^{-A[y_{cl}(t)]}\left(y_T^{\frac{1}{2-\alpha}}-E\right)\mathrm{d}y_T \tag{40}$$

which unfortunately is not possible to evaluate analytically, but it can be easily computed numerically for any conventional integration method.

5. Numerical simulations

We compute numerically, using a standard method (global adaptive quadrature [67]), the integral defined in Eq. (40). We also compute the pricing for the same European call option using the Schroder approach that considers the non-central chi-square distribution and set it as the benchmark.

We examine the results of both models, in terms of the pricing and the running time of each computation; considering several volatilities and elasticities of variances. Besides we test our results for short-time maturities ($T=\{0.25,0.5\}$) and long time maturities ($T=\{2,4\}$). In all the experiments we assume $r=0.05$, $S_0=100$ and $E=110$,

Firstly, we consider a maturity equal to six months. In Table 1 both the pricing and computational time (obtained as the average time for 1000 tries) are reported. We can see that the path integral method has similar pricing values but with a clear advantage in the running time. The times observed in Table 1 for the proposed method of path integral are always lower to 0.0011 s; however, for the non-central chi-square approach, the times are at least greater by 30 times. For a high value in the elasticity parameter and low volatility, the difference in time achieves two orders of magnitude.

For a clearer and complete view, we present the continuous results in Figs. 1, 2, and 3. The pricing and the running time are shown for both models sweeping on values of α. The figures confirm the observed concussions in Table 1 in the sense that the running times of the proposed method of path integral are significantly lower (right-hand side figures) than the traditional solution methodology for the CEV model, especially when α tends to 2 where the time of the benchmark

Table 1
Comparison of pricing and computational time for a Call option for some values of σ and α, using $T = 0.5$, $S_0 = 100$ and $E = 110$.

σ	α	Path integral		Benchmark	
		Pricing ($)	Time (s)	Pricing ($)	Time (s)
20%	1	$4.4289 \cdot 10^{-8}$	0.0009	$4.6567 \cdot 10^{-8}$	0.1407
	1.45	0.0580	0.0010	0.0600	0.0849
	1.9	1.8505	0.0011	1.8706	0.1888
50%	1	0.0259	0.0008	0.0275	0.0466
	1.45	1.3437	0.0009	1.4181	0.0298
	1.9	8.0777	0.0011	8.2636	0.0598
90%	1	0.3847	0.0010	0.4148	0.0246
	1.45	3.9003	0.0011	4.2358	0.0158
	1.9	16.4965	0.0010	17.1870	0.0362

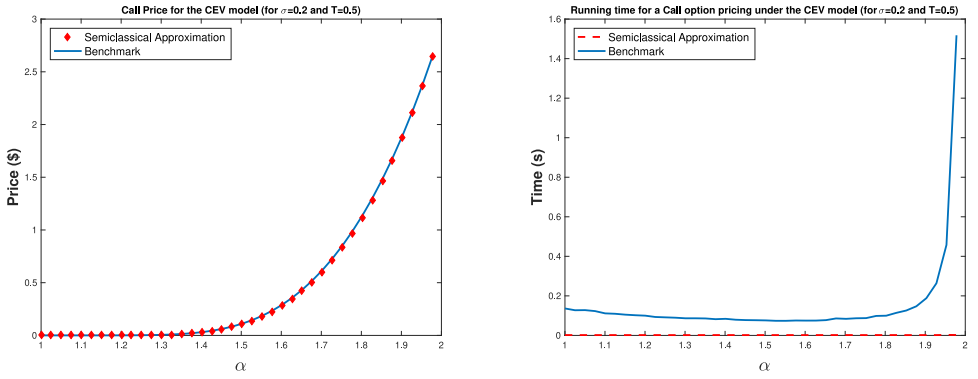

(a) Option Pricing (b) Running time

Fig. 1. Pricing and computational time for a Call option using σ =20%, $T = 0.5$, $r = 0.05$, $S_0 = 100$ and $E = 110$.

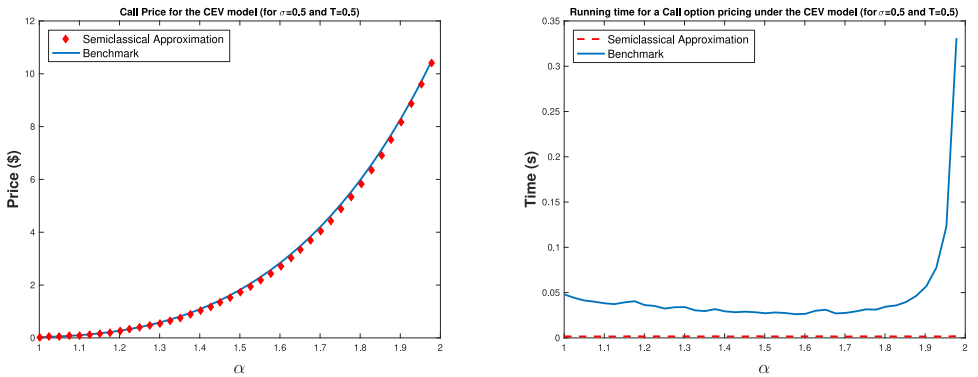

(a) Option Pricing (b) Running time

Fig. 2. Pricing and computational time for a Call option using σ =50%, $T = 0.5$, $r = 0.05$, $S_0 = 100$ and $E = 110$.

method rises considerably. In terms of accuracy, we can see that the path integral method fits very well in all cases. In order to have an estimation of the path integral approach, in Fig. 4 the absolute and relative errors are shown for several values of α and σ. Always, the relative error is no longer that 10% for the assumed parameters.

If we use a lower time to maturity (three months) the results in terms of computational time are very similar to the case $T = 0.5$ (although the time of the benchmark grows a little), and the fit is still good too. In fact, for lower maturity the path integral method performs better because the error is no greater than 2%. This is showed from Figs. 5 to 8.

For greater times to maturity, we have a change in the results, indicating the limits of the semiclassical approximation. For a two years maturity Figs. 9–12 we find results very similar to that of the previous cases, but with a more deviation in the pricing (absolute error). Still, the relative error remains lower than 12%. In terms of running time, the semiclassical approach performs similarly than in previous cases. While for the option pricing, we confirm the fact that there is a

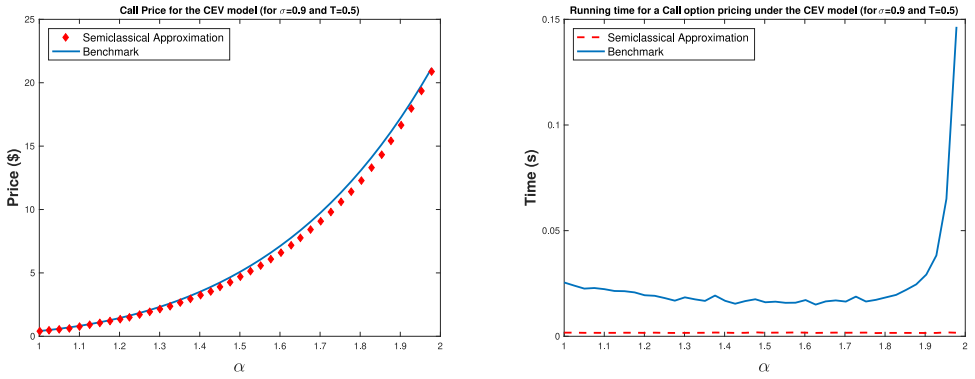

(a) Option Pricing (b) Running time

Fig. 3. Pricing and computational time for a Call option using σ =90%, $T = 0.5$, $r = 0.05$, $S_0 = 100$ and $E = 110$.

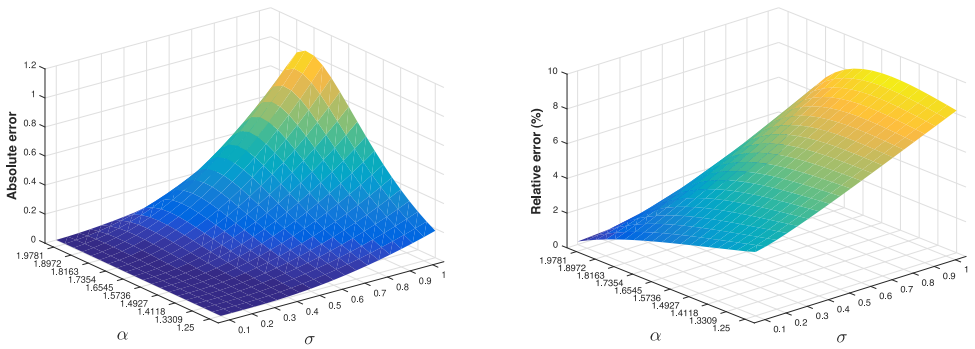

(a) Absolute error (b) Relative error

Fig. 4. Absolute and relative error of the path integral approach with $T = 0.5$, $r = 0.05$, $S_0 = 100$ and $E = 110$.

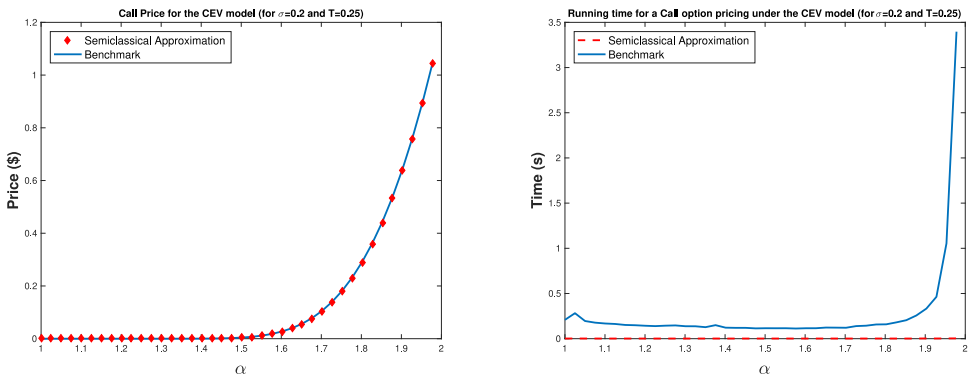

(a) Option Pricing (b) Running time

Fig. 5. Pricing and computational time for a Call option using σ =20%, $T = 0.25$, $r = 0.05$, $S_0 = 100$ and $E = 110$.

decline in time for both greater maturities and volatilities. However, the rising running times continue for α near two, and a significative time difference keeps in favor of the proposed method. This fact is confirmed when we use maturity equals to 4 years. In the same way, the pricing error goes up, despite the fact that the relative error remains under 20% (see Figs. 13–16).

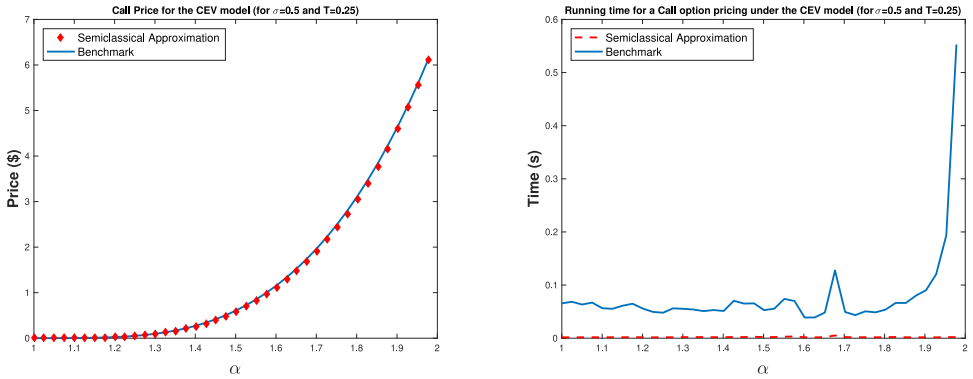

(a) Option Pricing (b) Running time

Fig. 6. Pricing and computational time for a Call option using σ =50%, $T = 0.25$, $r = 0.05$, $S_0 = 100$ and $E = 110$.

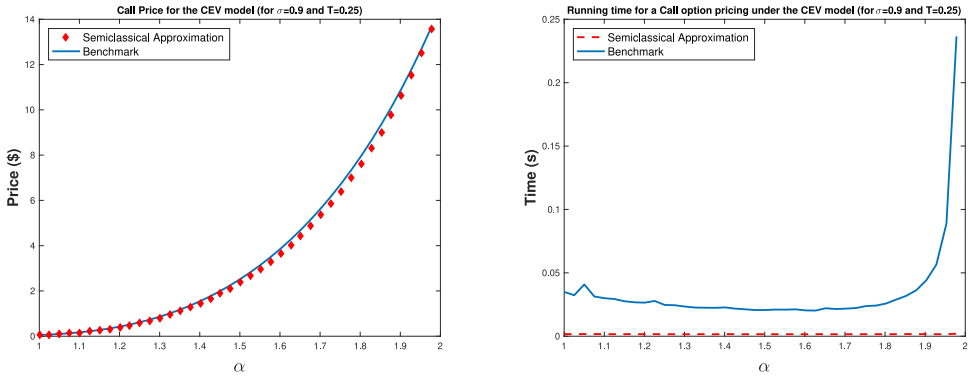

(a) Option Pricing (b) Running time

Fig. 7. Pricing and computational time for a Call option using σ =90%, $T = 0.25$, $r = 0.05$, $S_0 = 100$ and $E = 110$.

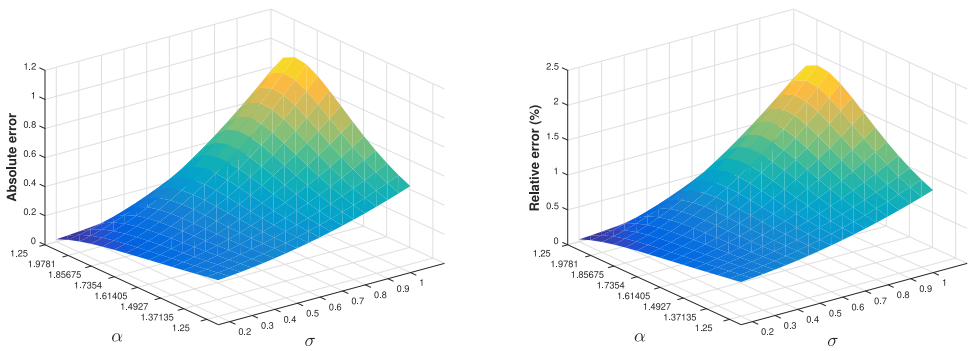

(a) Absolute error (b) Relative error

Fig. 8. Absolute and relative error of the path integral approach with $T = 0.25$, $r = 0.05$, $S_0 = 100$ and $E = 110$.

5.1. Comparison with other standard numerical methods

In order to compare the proposed semiclassical method with other standard numerical schemes, we have computed the Call-CEV option prices and their running times for the Monte Carlo, Binomial tree, and finite differences methods. In the tables below, we show the pricing and running times under the numerical approaches pointed out above for the same set of parameters given in Table 1. We report ΔMAPE (mean absolute percentage error) and Δ Time estimations for all models. ΔMAPE is defined as the difference between the MAPE of the method in question and the MAPE of the semiclassical method. Every MAPE is estimated with respect to the benchmarking, (non-central chi-squared). The same

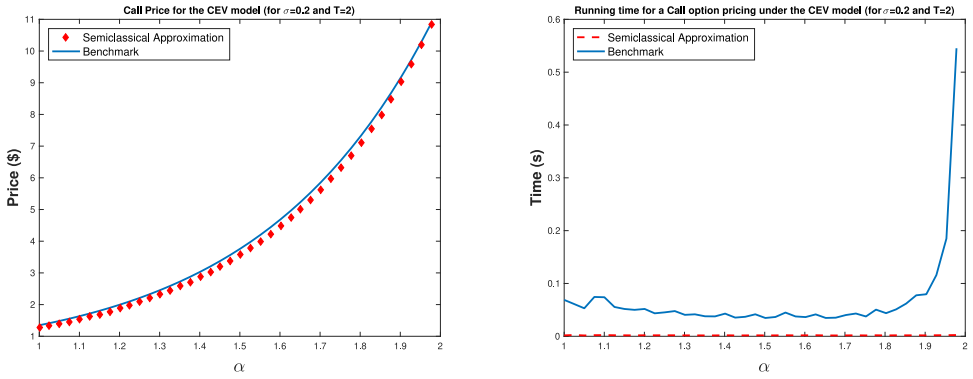

(a) Option Pricing (b) Running time

Fig. 9. Pricing and computational time for a Call option using $\sigma = 20\%$, $T = 2$, $r = 0.05$, $S_0 = 100$ and $E = 110$.

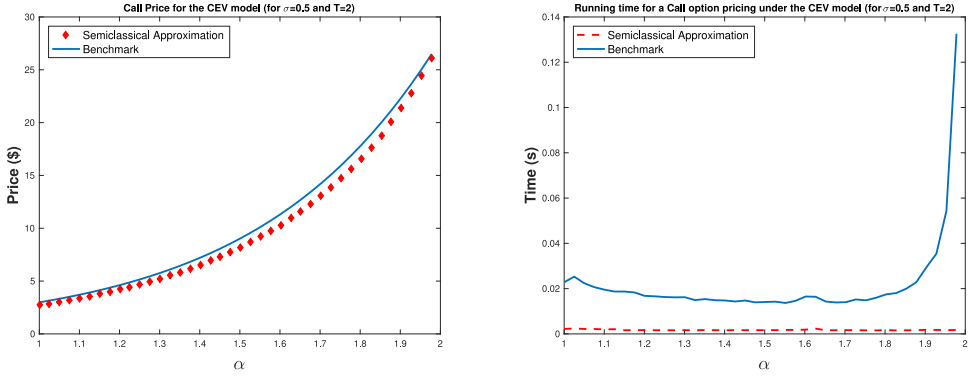

(a) Option Pricing (b) Running time

Fig. 10. Pricing and computational time for a Call option using $\sigma = 50\%$, $T = 2$, $r = 0.05$, $S_0 = 100$ and $E = 110$.

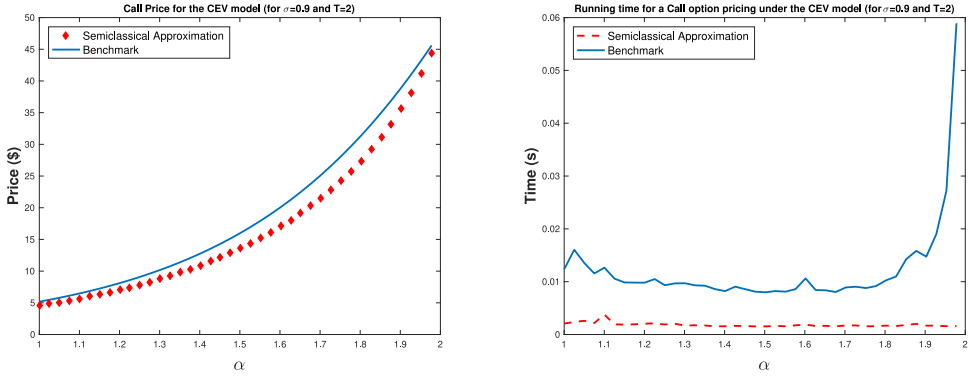

(a) Option Pricing (b) Running time

Fig. 11. Pricing and computational time for a Call option using σ =90%, $T = 2$, $r = 0.05$, $S_0 = 100$ and $E = 110$.

for the Δ Time estimations. It is defined as the difference between the running time of the method in question and the running time of the semiclassical method. In this context, a positive ΔMAPE means that the error is lower for the semiclassical method. Similarly, a positive Δ Time means that the running time is lower for the semiclassical method.

Table 2 displays the pricing and time for a Monte Carlo method (which simulate 10^4 and 10^5 values for S_T, and a standard Euler–Maruyama discretization). While the running times of the Montecarlo with 1000 simulations are clearly greater than the semiclassical times, the accuracy of Monte Carlo is poorer. These results do not change when we increase the number of simulations by a factor of 10.

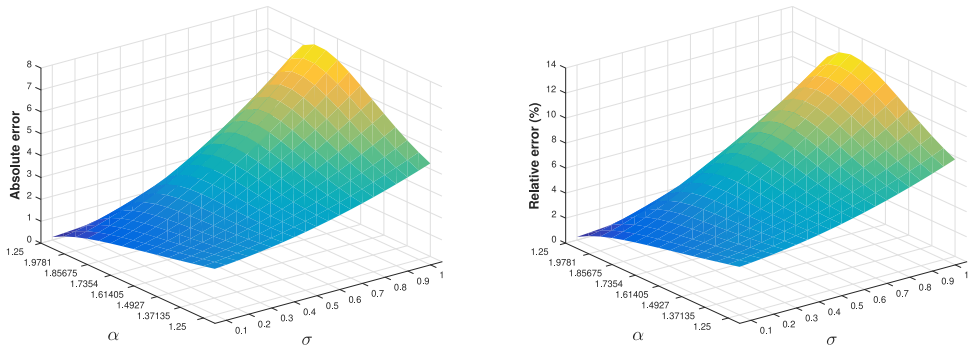

(a) Absolute error (b) Relative error

Fig. 12. Absolute and relative error of the path integral approach with $T = 2$, $r = 0.05$, $S_0 = 100$ and $E = 110$.

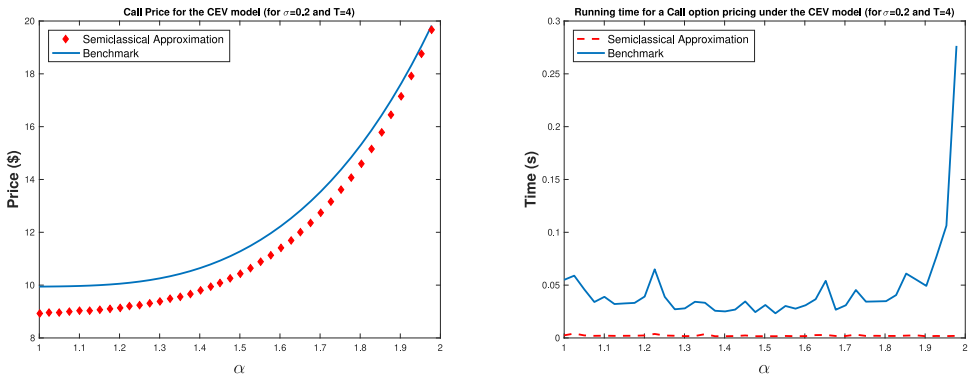

(a) Option Pricing (b) Running time

Fig. 13. Pricing and computational time for a Call option using $\sigma = 20\%$, $T = 4$, $r = 0.05$, $S_0 = 100$ and $E = 110$.

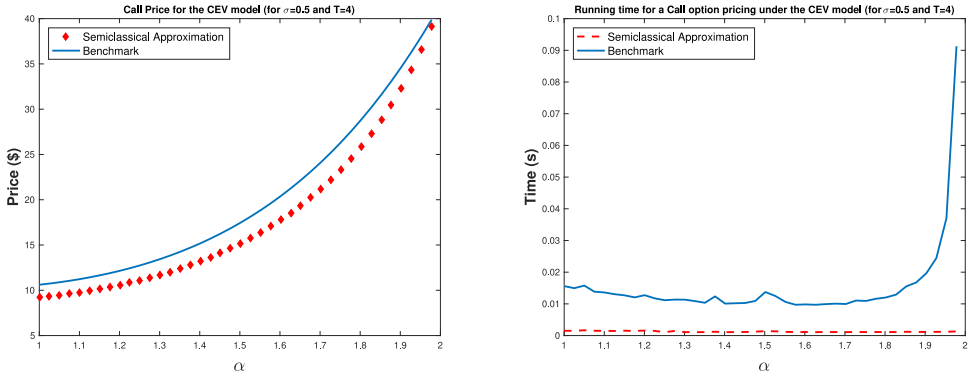

(a) Option Pricing (b) Running time

Fig. 14. Pricing and computational time for a Call option using $\sigma = 50\%$, $T = 4$, $r = 0.05$, $S_0 = 100$ and $E = 110$.

In order to value a European Call option by a binomial tree, we use the standard recombinant lattice scheme for the CEV model (see, for example, section 2.2 of Ref. [33]). Table 3 provides the pricing by a binomial tree using both 50 and 100 steps. The 50 steps binomial tree offers better results in terms of accuracy than the semiclassical method for higher volatilities, but greater execution times. If we increase the steps to 100 in the binomial tree, there is an improvement in the accuracy of the method compare to the semiclassical approximation, but the running time rises considerably.

Finally, in Table 4, the option pricing is obtained by an explicit finite difference method. We consider two lattices: one of 100 values for the asset and 2500 for the time, and another of 200 values for the asset and 9000 for the time. The asset values are restricted to the interval [0,200]. The time grid was selected as the lower value to avoid instability

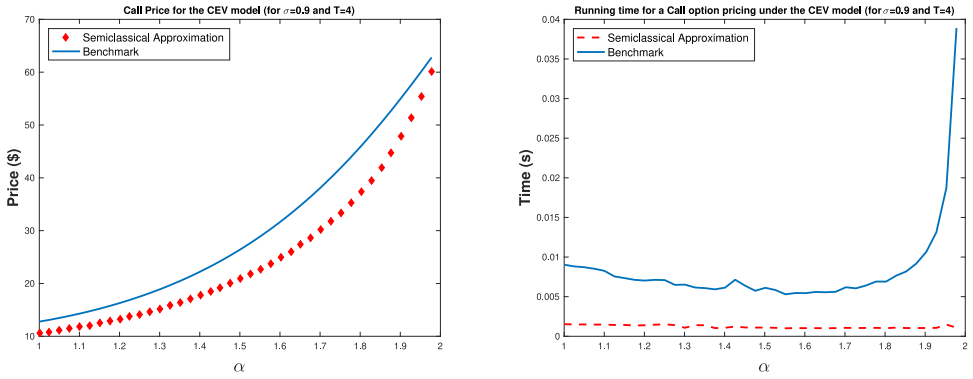

(a) Option Pricing (b) Running time

Fig. 15. Pricing and computational time for a Call option using $\sigma = 90\%$, $T = 4$, $r = 0.05$, $S_0 = 100$ and $E = 110$.

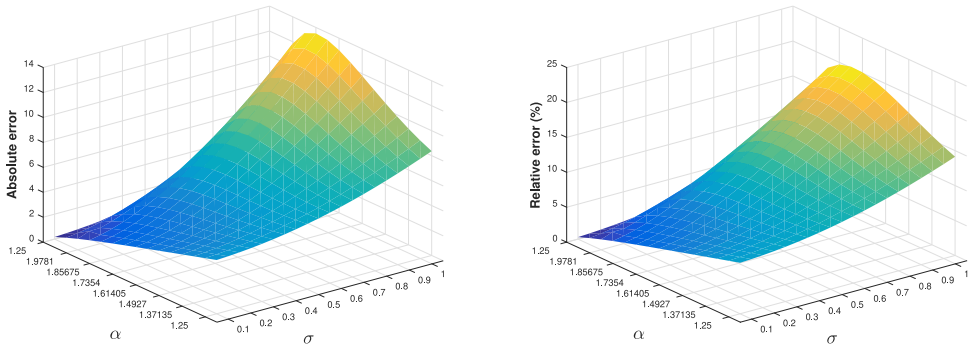

(a) Absolute error (b) Relative error

Fig. 16. Absolute and relative error of the path integral approach with $T = 4$, $r = 0.05$, $S_0 = 100$ and $E = 110$.

Table 2
Pricing and computational time, by Binomial Tree, for a Call option for some values of σ and α, using $T = 0.5$, $S_0 = 100$ and $E = 110$.

σ	α	Monte Carlo (10^4 iterations)		Monte Carlo (10^5 iterations)	
		Δ MAPE (%)	Δ Time (s)	Δ MAPE (%)	Δ Time (s)
20%	1	95.1	0.0006	53.0	0.0185
	1.45	21.8	0.0015	21.5	0.0227
	1.9	10.5	0.0016	10.6	0.0254
50%	1	18.2	0.0010	17.8	0.0154
	1.45	5.3	0.0017	5.3	0.0230
	1.9	5.1	0.0015	5.1	0.0236
90%	1	5.2	0.0006	5.0	0.0170
	1.45	−0.6	0.0017	−0.6	0.0245
	1.9	1.5	0.0016	1.6	0.0234

in all the cases described in Table 4, for a given asset discretization. Although the results are similar to the semiclassical method, the time-cost is higher for the 2500×100 finite difference scheme. Indeed, if we increase the resolution of the grid (9000×200), the accuracy rises, but also the execution times.

In graphical terms, in Figs. 17–19; the numerical methods addressed above, are compared with the non-central chi-squared approach (pricing) and the semiclassical approach (times); for a 3-month maturity, volatility equal to 20%, and elasticity parameter in the interval [1, 2]. These plots are contrasted with Fig. 5. We could see that the Monte Carlo method (Fig. 17) presents higher deviations from the benchmark, and their running times are greater than the semiclassical ones. In contrast, the binomial tree and finite difference methods, with small grid resolution, are competitive to the semiclassical approach in both accuracy and running times. In Fig. 18 we could see that the 50-step binomial tree offers similar times and pricing values than the semiclassical method. For the finite difference method, we plot (Fig. 19) the results using the lattices 2500 × 100 and 300 × 100. Even that a time grid off 300 points yields to unstable results for higher maturities and

Table 3
Pricing and computational time, by Binomial Tree, for a Call option for some values of σ and α, using $T = 0.5$, $S_0 = 100$ and $E = 110$.

σ	α	Binomial tree (50 steps)		Binomial tree (100 steps)	
		Δ MAPE (%)	Δ Time (s)	Δ MAPE (%)	Δ Time (s)
20%	1	95.1	0.0008	86.0	0.0032
	1.45	3.2	0.0007	1.7	0.0038
	1.9	0.3	0.0006	−1.0	0.0037
50%	1	6.5	0.0008	0.7	0.0031
	1.45	−4.8	0.0007	−5.0	0.0036
	1.9	−2.1	0.0005	−2.0	0.0036
90%	1	−6.5	0.0007	−6.8	0.0032
	1.45	−7.6	0.0006	−7.7	0.0036
	1.9	−3.6	0.0007	−3.8	0.0036

Table 4
Pricing and computational time, by Binomial Tree, for a Call option for some values of σ and α, using $T = 0.5$, $S_0 = 100$ and $E = 110$.

σ	α	Finite difference (2500×100)		Finite difference (9000×200)	
		Δ MAPE (%)	Δ Time (s)	Δ MAPE (%)	Δ Time (s)
20%	1	2709376.4	0.0170	120044.6	0.1226
	1.45	27.7	0.0168	3.0	0.1235
	1.9	−1.3	0.0159	−0.9	0.1317
50%	1	61.0	0.0172	8.4	0.1220
	1.45	3.5	0.0166	−5.1	0.1227
	1.9	−6.0	0.0164	−2.1	0.1317
90%	1	7.6	0.0164	−7.2	0.1210
	1.45	4.5	0.0159	−7.9	0.1222
	1.9	−14.1	0.0163	−2.3	0.2173

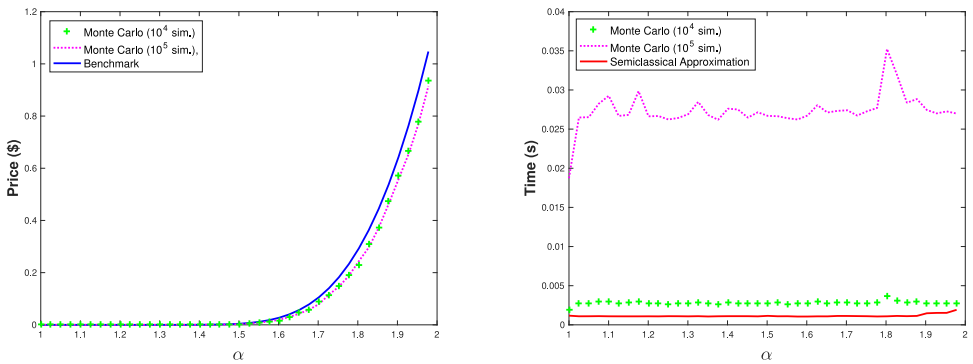

(a) Option Pricing (b) Running times

Fig. 17. Pricing and running times for the Monte Carlo approach with T = 0.25, $\sigma = 0.25$, $r = 0.05$, S_0 = 100 and E = 110.

volatilities, for $\sigma = 20\%$ and $T = 0.25$, the explicit scheme arrives at feasible results. Precisely, that lattice (300×100) offers competitive results to the semiclassical method.

Summing up, as expected the better performance of the semiclassical approximation is achieved at both lower maturities and volatilities.

6. Summary and further research

In this paper, a new numerical method for computing the CEV model was developed. In particular, this new approach was based on the semiclassical approximation of Feynman's path integral model. This formulation dealt with some of the limitations of the conventional approach based on the non-central chi-squared distribution.

The experimental results showed a good fit between the newly proposed method and the traditional methodology (setting the former as the benchmark), and also a lower computational cost, measured as the running time of each model.

We analyze several hypothetical scenarios, using different maturities, volatilities, and elasticities. In most cases, the running time is one order of magnitude lower than the benchmark, but if the elasticity tends to one, this difference is

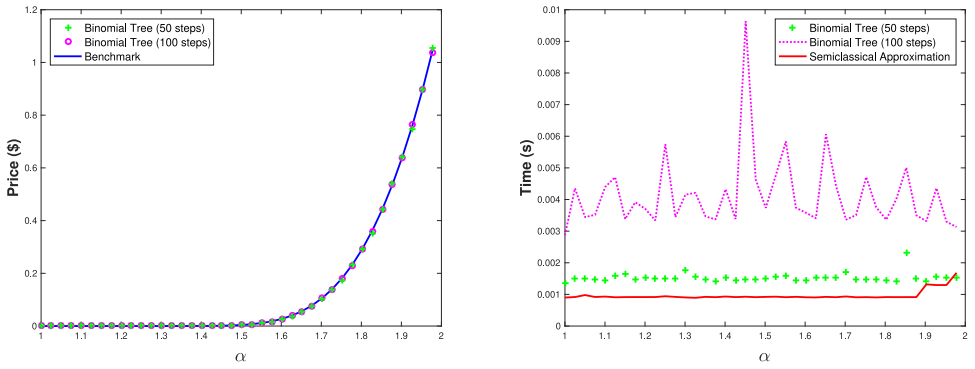

(a) Option pricing (b) Running times

Fig. 18. Pricing and running times for the binomial tree approach with T = 0.25, $\sigma = 0.25$, $r = 0.05$, S_0 = 100 and E = 110.

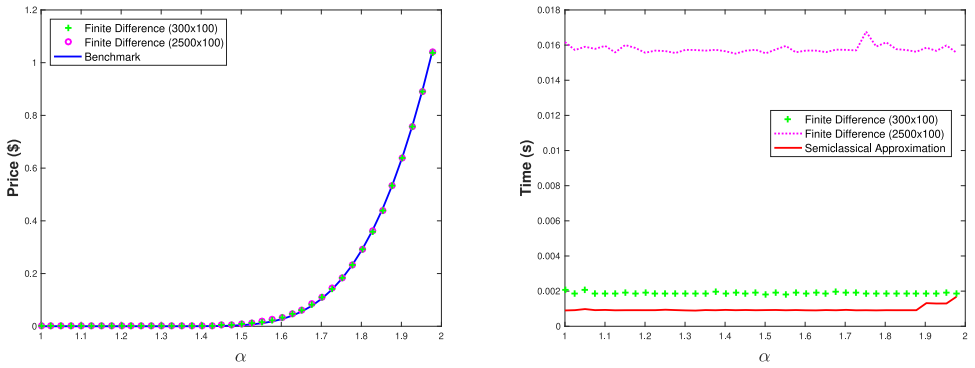

(a) Option pricing (b) Running times

Fig. 19. Pricing and running times for the finite difference approach with T = 0.25, $\sigma = 0.25$, $r = 0.05$, S_0 = 100 and E = 110.

higher. As an accuracy measure, the absolute and relative errors are computed. For the range $10\% < \sigma < 100\%$ and $1.25 < \alpha < 1.97$ the relative error is below 20% in all the cases. Nevertheless, for short maturities and lower volatilities, the error decreases considerably, coming to be less than 10% for small maturities (under 2% for T=0.25!) and for $\sigma < 50$.

The main remark is that this novel methodology allows the evaluation of a European contract under the CEV model computing only an integral without any complex numerically method. The accuracy and efficiency of this method positions it as a great competitor for the conventional methods based on the non-central chi-squared distribution, especially for lower volatilities and maturities. It also offers advantages over other standard numerical methods (namely Monte Carlo, binomial tree, and finite difference), with lower times of calculation considering similar levels of accuracy. Besides, it offers an analytical form for the transition density function; capability not addressed by its competitors.

In terms of future research, a natural first extension of the paper is to adopt the proposed methodology to American options. Also, the pricing of exotic options would be a good target. Another interesting research line is to apply the semiclassical approximation of Feynman's path integral model to more sophisticated stochastic volatility models such as Heston, SABR or GARCH type models, where the traditional current solutions are much more complicated than that of the CEV model, and hence the potential value-added of this methodology could be greater.

Acknowledgments

A. Araneda thanks the support from Operational Programme Research, Development and Education - Project "Postdoc2MUNI" (No. CZ.02.2.69/0.0/0.0/18_053/0016952).

References

[1] Fischer Black, Myron Scholes, The pricing of options and corporate liabilities, J. Polit. Econ. 81 (3) (1973) 637–654.
[2] Geert Bekaert, Guojun Wu, Asymmetric volatility and risk in equity markets, Rev. Financ. Stud. 13 (1) (2000) 1–42.
[3] Tim Bollerslev, Julia Litvinova, George Tauchen, Leverage and volatility feedback effects in high-frequency data, J. Financ. Econ. 4 (3) (2006) 353–384.

[4] Mark Rubinstein, Nonparametric tests of alternative option pricing models using all reported trades and quotes on the 30 most active CBOE option classes from August 23, 1976 through August 31, 1978, J. Finance 40 (2) (1985) 455–480.
[5] Jens Carsten Jackwerth, Mark Rubinstein, Recovering probability distributions from option prices, J. Finance 51 (5) (1996) 1611–1631.
[6] Robert F. Engle, Autoregressive conditional heteroscedasticity with estimates of the variance of United Kingdom inflation, Econometrica (1982) 987–1007.
[7] Tim Bollerslev, Ray Y. Chou, Kenneth F. Kroner, ARCH modeling in finance: A review of the theory and empirical evidence, J. Econometrics 52 (1–2) (1992) 5–59.
[8] Eric Ghysels, Andrew C. Harvey, Eric Renault, Stochastic volatility, in: G.S. Maddala, C.R. Rao (Eds.), Statistical Methods in Finance, in: Handbook of Statistics, vol. 14, Elsevier, 1996, pp. 119–191 (Chapter 5).
[9] Neil Shephard, Torben G. Andersen, Stochastic volatility: origins and overview, in: Thomas Mikosch, Jens-Peter Kreiß, Richard A. Davis, Torben Gustav Andersen (Eds.), Handbook of Financial Time Series, Springer, Berlin, Heidelberg, 2009, pp. 233–254.
[10] David G. Hobson, Leonard C.G. Rogers, Complete models with stochastic volatility, Math. Finance 8 (1) (1998) 27–48.
[11] John C. Cox, Notes on option pricing I: Constant elasticity of variance diffusions, Working paper, Stanford University, 1975.
[12] John C. Cox, The constant elasticity of variance option pricing model, J. Portf. Manag. 23 (5) (1996) 15–17.
[13] Weipeng Yuan, Shaoyong Lai, The CEV model and its application to financial markets with volatility uncertainty, J. Comput. Appl. Math. 344 (2018) 25–36.
[14] Weipeng Yuan, Shaoyong Lai, Family optimal investment strategy for a random household expenditure under the CEV model, J. Comput. Appl. Math. 354 (2019) 1–14.
[15] Stan Beckers, The constant elasticity of variance model and its implications for option pricing, J. Finance 35 (3) (1980) 661–673.
[16] Mark Schroder, Computing the constant elasticity of variance option pricing formula, J. Finance 44 (1) (1989) 211–219.
[17] Dmitry Davydov, Vadim Linetsky, Pricing and hedging path-dependent options under the CEV process, Manage. Sci. 47 (7) (2001) 949–965.
[18] Min Chen, Equity volatility smile and skew under a CEV-based structural leverage model, Appl. Math. Inf. Sci. 9 (3) (2015) 1095–1104.
[19] James D. MacBeth, Larry J. Merville, Tests of the Black–Scholes and Cox Call Option Valuation Models, J. Finance 35 (2) (1980) 285–301.
[20] David C. Emanuel, James D. MacBeth, Further results on the constant elasticity of variance call option pricing model, J. Financ. Quant. Anal. 17 (4) (1982) 533–554.
[21] Alan L. Tucker, David R. Peterson, Elton Scott, Tests of the black-scholes and constant elasticity of variance currency call option valuation models, J. Financ. Res. 11 (3) (1988) 201–214.
[22] Beni Lauterbach, Paul Schultz, Pricing warrants: An empirical study of the Black–Scholes model and its alternatives, J. Finance 45 (4) (1990) 1181–1209.
[23] V.K. Singh, N. Ahmad, Forecasting performance of constant elasticity of variance model: Empirical evidence from India, Int. J. Appl. Econ. Finance 5 (1) (2011) 87–96.
[24] K.C. Yuen, H. Yang, K.L. Chu, Estimation in the constant elasticity of variance model, Br. Actuar. J. 7 (2) (2001) 275–292.
[25] Ying-Lin Hsu, T.I. Lin, C.F. Lee, Constant elasticity of variance (CEV) option pricing model: Integration and detailed derivation, Math. Comput. Simulation 79 (1) (2008) 60–71.
[26] Manuela Larguinho, José Carlos Dias, Carlos A. Braumann, On the computation of option prices and Greeks under the CEV model, Quant. Finance 13 (6) (2013) 907–917.
[27] Sihun Jo, Minsuk Yang, Geonwoo Kim, On convergence of Laplace inversion for the American put option under the CEV model, J. Comput. Appl. Math. 305 (2016) 36–43.
[28] Shengliang Zhang, Hongqiang Yang, Yu Yang, A multiquadric quasi-interpolations method for CEV option pricing model, J. Comput. Appl. Math. 347 (2019) 1–11.
[29] Nawdha Thakoor, Désiré Yannick Tangman, Muddun Bhuruth, A new fourth-order numerical scheme for option pricing under the CEV model, Appl. Math. Lett. 26 (1) (2013) 160–164.
[30] Nawdha Thakoor, Désiré Yannick Tangman, Muddun Bhuruth, Fast valuation of CEV American options, Wilmott 2015 (75) (2015) 54–61.
[31] Richard Lu, Yi-Hwa Hsu, Valuation of standard options under the constant elasticity of variance model, Int. J. Bus. Econ. 4 (2) (2005) 157.
[32] Rajae Aboulaich, Abdelilah Jraifi, Ibtissam Medarhri, Stochastic Runge Kutta methods with the Constant Elasticity of Variance (CEV) diffusion model for pricing option, Int. J. Math. Anal. 8 (18) (2014) 849–856.
[33] Aricson Cruz, José Carlos Dias, The binomial CEV model and the Greeks, J. Futures Mark. 37 (1) (2017) 90–104.
[34] A.E. Lindsay, D.R. Brecher, Simulation of the CEV process and the local martingale property, Math. Comput. Simulation 82 (5) (2012) 868–878.
[35] Sang-Hyeon Park, Jeong-Hoon Kim, Asymptotic option pricing under the CEV diffusion, J. Math. Anal. Appl. 375 (2) (2011) 490–501.
[36] Stefano Pagliarani, Andrea Pascucci, Analytical approximation of the transition density in a local volatility model, Cent. Eur. J. Math. 10 (1) (2012) 250–270.
[37] Vladislav Krasin, Ivan Smirnov, Alexander Melnikov, Approximate option pricing and hedging in the CEV model via path–wise comparison of stochastic processes, Ann. Finance (2017) 1–15.
[38] Vadim Linetsky, The path integral approach to financial modeling and options pricing, Comput. Econ. 11 (1) (1997) 129–163.
[39] Guido Montagna, Oreste Nicrosini, Nicola Moreni, A path integral way to option pricing, Physica A 310 (3) (2002) 450–466.
[40] G. Bormetti, Guido Montagna, N. Moreni, Oreste Nicrosini, Pricing exotic options in a path integral approach, Quant. Finance 6 (1) (2006) 55–66.
[41] Belal E. Baaquie, Quantum Finance: Path Integrals and Hamiltonians for Options and Interest Rates, Cambridge University Press, 2007.
[42] D. Lemmens, M. Wouters, J. Tempere, S. Foulon, Path integral approach to closed-form option pricing formulas with applications to stochastic volatility and interest rate models, Phys. Rev. E 78 (1) (2008) 016101.
[43] Jeroen P.A. Devreese, Damiaan Lemmens, Jacques Tempere, Path integral approach to Asian options in the Black–Scholes model, Physica A 389 (4) (2010) 780–788.
[44] Mauricio Contreras, Rely Pellicer, Marcelo Villena, Aaron Ruiz, A quantum model of option pricing: When Black–Scholes meets Schrödinger and its semi–classical limit, Physica A 389 (23) (2010) 5447–5459.
[45] Mauricio Contreras, Rodrigo Montalva, Rely Pellicer, Marcelo Villena, Dynamic option pricing with endogenous stochastic arbitrage, Physica A 389 (17) (2010) 3552–3564.
[46] Richard Phillips Feynman, Space-time approach to non-relativistic quantum mechanics, Rev. Modern Phys. 20 (2) (1948) 367.
[47] Richard P. Feynman, Albert R. Hibbs, Quantum Mechanics and Path Integrals, Courier Corporation, Mineola, NY, 2010,
[48] Christian Grosche, Frank Steiner, Handbook of Feynman Path Integrals, Springer Tracts in Modern Physics, vol. 145, Springer, 1998.
[49] Hagen Kleinert, Path Integrals in Quantum Mechanics, Statistics, Polymer Physics, and Financial Markets, World Scientific, 2004.
[50] Paul A.M. Dirac, The Lagrangian in quantum mechanics, Phys. Z. Sowjetunion 3 (64) (1933) 64–72.
[51] Rf Rajaraman, Some non-perturbative semi-classical methods in quantum field theory (a pedagogical review), Phys. Rep. 21 (5) (1975) 227–313.
[52] Thijs Koeling, R.A. Malfliet, Semi–classical approximations to heavy ion scattering based on the Feynman path-integral method, Phys. Rep. 22 (4) (1975) 181–213.
[53] Zura Kakushadze, Path integral and asset pricing, Quant. Finance 15 (11) (2015) 1759–1771.
[54] Masud Chaichian, Andrei Demichev, Path Integrals in Physics: Stochastic Processes and Quantum Mechanics, Institute of Physics, 2001.

[55] Cécile Morette, On the definition and approximation of Feynman's path integrals, Phys. Rev. 81 (5) (1951) 848.
[56] Cécile DeWitt-Morette, Feynman path integrals, Comm. Math. Phys. 37 (1) (1974) 63–81.
[57] P. Choquard, F. Steiner, The story of Van Vleck's and Morette Van Hove's determinants, Helv. Phys. Acta 69 (5–6) (1996) 636–654.
[58] John H. Van Vleck, The correspondence principle in the statistical interpretation of quantum mechanics, Proc. Natl. Acad. Sci. 14 (2) (1928) 178–188.
[59] Hannen Risken, The Fokker–Planck Equation, first ed., Springer Series in Synergetics, vol. 18, Springer, 1984.
[60] Belal E. Baaquie, Claudio Coriano, Marakani Srikant, Hamiltonian and potentials in derivative pricing models: exact results and lattice simulations, Physica A 334 (3) (2004) 531–557.
[61] Dirk Veestraeten, On the multiplicity of option prices under CEV with positive elasticity of variance, Rev. Deriv. Res. 20 (1) (2017) 1–13.
[62] Freddy Delbaen, Hiroshi Shirakawa, A note on option pricing for the constant elasticity of variance model, Asia-Pac. Financ. Mark. 9 (2) (2002) 85–99.
[63] Matthew Lorig, The exact smile of certain local volatility models, Quant. Finance 13 (6) (2013) 897–905.
[64] Axel A. Araneda, The fractional and mixed-fractional CEV model, J. Comput. Appl. Math. 363 (2020) 106–123.
[65] John C. Cox, Stephen A. Ross, The valuation of options for alternative stochastic processes, J. Financ. Econ. 3 (1–2) (1976) 145–166.
[66] George E. Uhlenbeck, Leonard S. Ornstein, On the theory of the Brownian motion, Phys. Rev. 36 (5) (1930) 823.
[67] Lawrence F. Shampine, Vectorized adaptive quadrature in MATLAB, J. Comput. Appl. Math. 211 (2) (2008) 131–140.